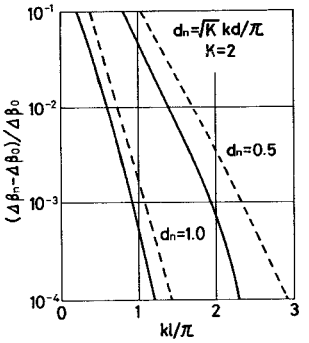

Fig. 8. Accuracy of the proposed method in comparison with a rigorous solution.

surrounding medium. The solid lines show $(\Delta\beta_1 - \Delta\beta_0)/\Delta\beta_0$ while the broken lines show $(\Delta\beta_2 - \Delta\beta_0)/\Delta\beta_0$, both as a function of the normalized frequency (or the normalized separation distance). As we can see from Fig. 8, the accuracy of the proposed method is satisfactorily good. The accuracy becomes excellent as the separation l increases, or the frequency becomes higher (in other words, the amount of the power transmitted within each guide increases).

REFERENCES

[1] M. F. Bracey, A. L. Cullen, E. F. F. Gillespie, and J. A. Staniforth, "Surface-wave research in Sheffield," *IRE Trans. Antennas Propagat. (Special Supplement)*, vol. AP-7, pp. S219–225, Dec. 1959.
[2] A. L. Jones, "Coupling of optical fibers and scattering in fibers," *J. Opt. Soc. Amer.*, vol. 55, p. 261, Mar. 1965.
[3] E. A. J. Marcatili, "Dielectric rectangular waveguide and directional coupler for integrated optics," *Bell Syst. Tech. J.*, vol. 48, p. 2071, Sept. 1969.
[4] R. Vanclooster and P. Phariseau, "The coupling of two parallel dielectric fibers—I: Basic equations," *Physica*, vol. 47, p. 485, June 1970.
[5] D. Marcuse, "The coupling of degenerate modes in two parallel dielectric waveguides," *Bell Syst. Tech. J.*, vol. 50, p. 1791, July 1971; see also *Light Transmission Optics*. New York: Van Nostrand, 1972, ch. 10.
[6] A. W. Snyder, "Coupled-mode theory for optical fibers," *J. Opt. Soc. Amer.*, vol. 62, p. 1267, Nov. 1972.
[7] K. Kurokawa, "Electromagnetic waves in waveguides with wall impedance," *IRE Trans. Microwave Theory Tech.*, vol. MTT-10, pp. 314–320, Sept. 1962.
[8] D. Marcuse, *Light Transmission Optics*. New York: Van Nostrand, 1972, ch. 7.
[9] S. E. Miller, "Coupled wave theory and waveguide applications," *Bell Syst. Tech. J.*, vol. 33, p. 661, May 1954.

An S-Band Radiometer Design with High Absolute Precision

WALTER N. HARDY, KENNETH W. GRAY, AND A. W. LOVE, MEMBER, IEEE

Abstract—A radiometer for the remote measurement of sea surface temperature is described. Two requirements are necessary for the attainment of an absolute accuracy of 1 or 2 K in molecular temperature. Although the first is inappropriate for discussion here, it is clear that corrections must be developed to account for perturbations caused by surface effects (roughness, foaming, and salinity changes) and for atmospheric effects (absorption and scattering). The second requirement, namely, the development of an instrument capable not only of high relative accuracy (i.e., resolution) but also of high absolute precision, is the subject of this paper.

The concepts underlying the design of an instrument capable of an absolute accuracy of a few tenths degrees Kelvin in the measurement of brightness temperature at S band are described. The role of the antenna is discussed and the importance of high ohmic and beam efficiencies is stressed. The hardware itself is fully described, along with an outline on the design of a unique cryogenically cooled termination used to calibrate the whole radiometer, including antenna.

Finally, some test results are presented that show that the design goals for the instrument have been closely approached.

Manuscript received May 14, 1973; revised August 22, 1973. This work was supported by the NASA Langley Research Center under Contracts NAS1-10106 and NAS1-10691.

W. N. Hardy was with the Science Center, Rockwell International Corporation, Thousand Oaks, Calif. He is now with the Department of Physics, University of British Columbia, Vancouver, B. C., Canada.
K. W. Gray was with the Science Center, Rockwell International Corporation, Thousand Oaks, Calif. He is now with the Royal Radar Establishment, Great Malvern, Worcs., England.
A. W. Love is with the Space Division, Rockwell International Corporation, Downey, Calif.

I. INTRODUCTION AND BACKGROUND

OVER the past 25 years a wide variety of microwave radiometer configurations of varying complexity and sensitivity have been proposed. Although it is common practice in the literature to state the theoretical and experimental temperature resolution of a radiometer, there is almost a complete lack of information on the absolute accuracy achieved. There is a potential need for a spaceborne microwave radiometer to measure remotely the sea surface temperature, in which case it is necessary that the radiometric temperature be determined with a resolution of 0.1 K and with an absolute accuracy approaching ±0.1 K.

Antenna temperature resolutions of 0.1 K are routinely

achieved in microwave radiometers provided adequate predetection bandwidth is used. On the other hand, the requirement of long-term absolute accuracy of ±0.1 K is not easily satisfied and necessitates extreme care in the system design. Care in the design of the electronic circuitry, in the choice of microwave components, etc., is taken for granted. In addition, the high precision brings in practical difficulties of a more fundamental nature, such as the stability of reflective and dissipative transmission losses in the antenna and the input to the radiometer, and the absolute accuracy of the reference terminations. The development of a signal-modulated radiometer of the Dicke type [1] that meets these stringent requirements is reported here.

The detailed criteria for the selection of the operational frequency of the instrument are given elsewhere [2]. In essence, the choice of 2.65 GHz was a compromise between the perturbing effects of the atmosphere at high frequencies and the galactic background noise at low frequencies. It has been calculated from the measured values of the complex dielectric constant of sea water [2] that the emissivity at normal incidence varies only from 0.34 to 0.35 over the ranges 5–30°C in temperature and 30–36 parts/thousand in salinity. The radiometric temperature of the smooth sea at nadir in this frequency band is therefore very nearly proportional to its physical temperature and lies in the range 95–106 K. At this frequency, the major correction to the thermal radiation from the sea (under clear atmospheric conditions) is due to oxygen absorption, which contributes between 3.4 and 6.0 K depending on the altitude from which the sea is viewed.

The emissivity of the sea changes from its specular value when the surface is roughened by wave action. The accompanying increase in brightness temperature (average of the parallel and perpendicularly polarized emission components over an antenna beam of 0.1-sr solid angle) at *S* band has been observed to be 2.0 K or more, depending on surface conditions and viewing angle [2]. This is about an order of magnitude greater than is predicted by current theories that use the Kirchhoff approximation [3] to derive the emissive properties of the rough sea. In order to measure such perturbations experimentally and to assess the possibility of remotely measuring sea surface temperature to an accuracy of 1 or 2 K, it is clearly desirable to have a radiometer whose absolute accuracy approaches a few tenths degrees.

As a further design goal, the instrument is intended to be compatible with eventual unattended spacecraft use. Consequently, it requires a high degree of long-term stability and it does not rely upon the use of cryogenic liquids during operation. Although these are convenient for ground-based work, their use in a satellite presents difficulties. The preferred technique for space-borne calibration is to point the radiometer's antenna toward the galactic pole, where the sum of the cosmic and galactic background temperatures is constant and equal to 3.0 K at 2.65 GHz. The present uncertainty (±0.5°) in this value is certain to be substantially reduced in the near future.

II. BASIC DESIGN CONSIDERATIONS

A. Effect of Losses

Consider first the influence of RF losses on the absolute accuracy of a radiometer. Let the fractional ohmic loss (comprising antenna and all transmission line losses including the asymmetric part of the Dicke switch loss) be l, and suppose that all components contributing to this loss are at the same temperature T_0. Suppose further that there is a reflective discontinuity at, say, the antenna terminals having power reflection coefficient ρ. For small l and ρ the actual temperature seen by the radiometer T_a is related to T_A, the temperature of the radiation incident on the antenna, by

$$T_a \simeq (1 - l - \rho)T_A + lT_0 + \rho T_{\text{eff}} \quad (1)$$

where T_{eff} is the effective temperature of the power flowing in the reverse direction, i.e., from the receiver back through the Dicke switch to the antenna.

The temperature increase caused by the losses is given by

$$\Delta T = T_a - T_A = l(T_0 - T_A) + \rho(T_{\text{eff}} - T_A). \quad (2)$$

For a radiometer viewing the sea, T_A will be about 100 K while T_0 and T_{eff} might each be 300 K. Then even if the ohmic and mismatch losses are each only 0.001 dB, the resulting increase is nearly 0.1 K. In a practical radiometer, with losses of a decibel or more, the effect of the very much larger temperature increase is largely removed in the calibration procedure. Even so, it is still necessary to estimate and apply a correction for the fact that the loss is not the same when calibrating as it is when measuring a target.

The impracticality of this method becomes evident when an absolute accuracy approaching 0.1 K is desired. All losses, both reflective and dissipative, must then be relied upon to remain constant to order 0.001 dB. To achieve 0.1-K accuracy in the reference and calibrating terminations means that these devices must be primary standards of brightness temperature, for at this level of precision there is no way to calibrate them. The effective temperature of the load material must be determined in the presence of temperature gradients and, because (1) applies equally to this case (with T_A replaced by the physical temperature of the load), the distribution of both loss and temperature in the load and its associated transmission lines must be accurately known. Finally, as a matter of experience, the stability and repeatability of transmission line connectors cannot be relied upon to the level of 0.001 dB except under carefully controlled laboratory conditions.

B. Precision Comparator Concept

The approach that has been adopted is based upon the observation that no correction at all is required providing

T_0 and T_{eff} in (2) are equal to T_A. So long as this condition is obtained no errors will be introduced by either reflective or dissipative losses of any magnitude (large losses will degrade the sensitivity but will not affect accuracy) and the need for stability in the losses is eliminated. In the instrument to be described, the necessity for providing cryogenic cooling has been avoided by adding noise power to T_A in the antenna arm in order to bring the total input noise T_{in} up to the level of T_0.

The radiometer is, therefore, designed around the following two basic concepts.

1) The use of a constant-temperature enclosure at the same temperature T_0 as the main reference termination that, in conjunction with a nulling mode of operation, avoids the effects of time-dependent losses in the high-loss components such as the circulator switch.

2) The use of a pulsed noise source to provide variable noise injection. A constant pulsewidth is easy to achieve so that antenna temperature changes are accurately proportional to changes in pulse-repetition rate.

The advantages of maintaining the input components at a common temperature can be most easily understood by reference to Fig. 1. This shows the usual Dicke-type radiometer to which is added a noise injection arm and a constant-temperature enclosure that includes the reference termination. If the RF output is amplified, detected, and then demodulated at the switching frequency, then the condition for zero ac signal at the modulation frequency is exactly that $T_{\text{in}} = T_0$, the temperature of the enclosure. This result is completely independent of losses or reflections in the circulator switch, imperfections in the reference termination, finite switching times, etc., provided only that the isolator "isolates" well enough and that a single electromagnetic mode propagates in the input and output transmission lines. To see this, one need only imagine the input arm terminated with a load at the same temperature as the enclosure. Then, since all of the components including the circulator are passive and at common temperature T_0, by Nyquist's theorem [4], the power emitted at the output into each electromagnetic mode is given by (assuming for the moment that the isolator has zero reflection)

$$P_0 = kT_0B \tag{3}$$

which is strictly independent of time and which of course is totally independent of details of the components within the constant-temperature enclosure. This obviously satisfies the condition for ac null. Provided the amount of input signal reaching the output varies in some way with the switching state, then the condition $T_{\text{in}} \neq T_0$ results in an ac signal. The purpose of the isolator is to ensure that should there be a reflection looking into the output arm, it will remain constant. (The reflection coefficient of the circulator switch, for example, is different in general for its two states.) How well the isolator need isolate depends on the effective temperature T_{eff} seen looking towards the RF amplifier. If $\Delta\rho$ is the change in power reflection coefficient of the circulator, for example, and t the transmission coefficient of the isolator in the reverse direction, then the error in the radiometer output is given by

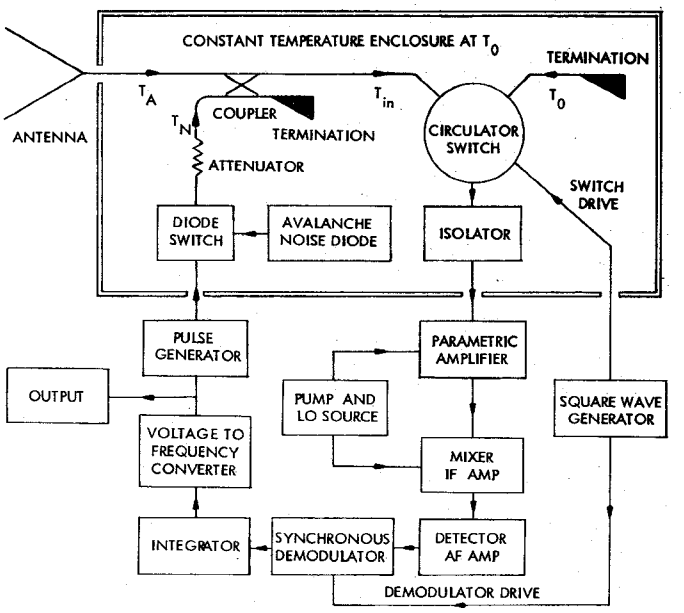

Fig. 1. Simplified block diagram.

$$\Delta T = (T_{\text{eff}} - T_0)t\Delta\rho. \tag{4}$$

For parametric or tunnel diode amplifiers that have circulator inputs, T_{eff} never deviates by more than a few degrees from ambient temperature. In an extreme case $\Delta\rho$ might be as large as 0.01; therefore, taking $T_{\text{eff}} - T_0 = 10$ K, $\Delta T = 0.001$ K, a completely negligible quantity, for a modest isolation of 20 dB ($t = 0.01$).

It is not necessary to restrict the input transmission line to single mode propagation, but the condition $T_{\text{in}} = T_0$ must then be satisfied for each mode. One further point is that, although in the above the circulator is assumed to be passive, this is not strictly true during switching. However, the switching rate of the ferrite is so much smaller than the microwave frequency that direct generation of microwaves can be completely ignored.

The radiometer operates in a feedback mode [5] whereby the injected noise power level is adjusted to achieve a null at the output, as indicated in the simplified block diagram of the complete radiometer shown in Fig. 1. By gating the noise with constant-width pulses, an extremely linear relationship between the pulse frequency f and the average injected noise is established. However, the null condition for the radiometer has to be reexamined for this mode of operation. It can be shown that if the detector is square law, then the condition for a null is exactly $\langle T_{\text{in}} \rangle_{\text{aver}} = T_0$, so that the advantages of the precision comparator are maintained. The effect of small departures from square law is treated in the Appendix.

III. THEORY

A. System Response

The operation of the radiometer may easily be followed by reference to Fig. 1. The output of the noise diode is

injected into the "comparator" input in the form of, for for example, 40-μs pulses. An error signal at the output of the demodulator causes the frequency of the pulses to vary in such a way as to reduce the error signal.

Applying the analysis of Seling [6], the feedback loop is imagined to be opened. Then the output of the voltage to frequency converter, Fig. 1, is a frequency f, given by

$$f = K'(T_0 - T_{\text{in}}) \tag{5}$$

where the transfer function K' depends upon the RF and IF gain, the square law detection sensitivity, the audio frequency (AF) gain, the demodulation and integrator characteristics, and the conversion sensitivity of the voltage to frequency converter. The dominant time constant is that of the integrator, all other elements having much faster response. Hence K' can be written

$$K' = \frac{K}{j\omega CR} \tag{6}$$

where K is the steady-state transfer characteristic and $(j\omega CR)^{-1}$ is the frequency response function of the assumed ideal integrator.

The diode gating switch, pulsed at the frequency f, establishes an average noise temperature at the directional coupler given by

$$\begin{aligned} T_N &= \tau f T_d + (1 - \tau f) T_0 \\ &= \tau f T_e + T_0 \end{aligned} \tag{7}$$

where τ is the pulsewidth, T_d is the temperature of the attenuated avalanche diode noise, and T_e is the excess noise temperature.

Closing the feedback loop results in

$$T_{\text{in}} = (1 - \beta) T_A + \beta T_N \tag{8}$$

where β is the coupling factor of the directional coupler. Substituting (6)–(8) in (5) then gives

$$f = \frac{k}{1 + j\omega(kCR/K(1 - \beta))} (T_0 - T_A) \tag{9}$$

in which the new steady-state transfer function k is given by

$$k = \frac{1 - \beta}{\beta \tau T_e} \tag{10}$$

and the frequency response is just that of a single resistance–capacitance filter section with time constant equal to $k/K(1 - \beta)$ times that of the integrator.

These results show that the steady-state stability and linearity of the system depend only on the coupling factor β and on the stability of the pulsewidth τ and the noise diode excess temperature T_e. Since the coupler is a purely passive element, housed in a temperature-regulated enclosure, its stability is extremely high. (The question of the stability of τ and T_e will be taken up in later sections.) Because gain variations affect only K, they have no effect on the average steady-state output, and for these conditions (9) becomes simply

$$f = k(T_0 - T_A). \tag{11}$$

The value of k is determined by calibration, which consists in measuring the pulse frequency f_c while a known temperature T_c is established at the antenna aperture. In this case the unknown antenna temperature becomes

$$\begin{aligned} T_A &= T_0 - \frac{f}{f_c}(T_0 - T_c) \\ &= \frac{f}{f_c} T_c + \left(1 - \frac{f}{f_c}\right) T_0. \end{aligned} \tag{12}$$

In practice the antenna is neither lossless nor perfectly matched and is physically too large to be regulated to the reference temperature T_0. This requires that a small correction term be added to the right side of (12). It is easy to show that the correction is given by

$$\Delta = \frac{l}{1 - l - R}\left[(T_0 - T_p) - \frac{f}{f_c}(T_0 - T_{pc})\right] \tag{13}$$

where l is the fractional ohmic loss in the antenna and R is the power reflection coefficient at its input. T_p and T_{pc} are the physical temperatures of the antenna under operating and calibrating conditions, respectively. In present usage of the radiometer, R is negligible and $l \simeq 0.02$, so that the magnitude of Δ seldom exceeds 0.2 K for normal temperature conditions.

B. Resolution

The sensitivity of the null-balanced feedback radiometer can be derived using the results of Tiuri [7]:

$$\Delta T_{\text{rms}} = 2\frac{T_0 + T_R}{1 - L}\left[\frac{2b}{B} + \left(\frac{\Delta G}{G}\right)^2\right]^{1/2} \tag{14}$$

where L is the fractional loss up to the paramp input, at which point the receiver noise temperature is T_R. The bandwidths B and b are the pre- and postdetection noise bandwidths, respectively. When the system response is that of a single-section RC filter, then $b = (4RC)^{-1}$; in this case the effective RC time constant given in (9) should be used. Finally, the term $\Delta G/G$ represents the fractional gain variations occurring at the modulation frequency. They are thought to be negligible for the present radiometer.

The effect of adding noise in the signal arm is to increase the output fluctuations over those of a conventional radiometer in the ratio

$$(T_0 + T_R)/(T_A + T_R).$$

The degenerate paramp used in this radiometer has a noise temperature of only 50 K, but contributions from later stages give an effective value $T_R = 70$ K. With $T_0 = 300$ K and $T_A = 110$ K, the above ratio is approximately 2.

IV. INSTRUMENTATION

A. Antenna

There is strong theoretical evidence that the average of the parallel and perpendicularly polarized components

of emission from the sea is considerably less sensitive to roughness than either component alone. An easy and convenient way to achieve such averaging is by use of an antenna sensitive to circular polarization over the whole of its main beam. Two additional antenna requirements of paramount importance for this application are low ohmic loss and exceptionally high beam efficiency, but aperture efficiency is only of secondary concern.

The only antenna capable of meeting all these requirements is some form of compensated horn, e.g., corrugated [8] or multimode [9], [10]. The latter has been selected for this application and the horn has a square aperture 14 in/side with a half-flare-angle of 6° 15′. In addition to the dominant TE_{10} mode, a hybrid mixture of TE_{12} and TM_{12} modes is generated near the throat of the horn by a discontinuous step in the square waveguide. When the modes are correctly proportioned and phased at the aperture, the normally large (−13-dB) E-plane sidelobes are suppressed to −30 dB, or more if desired. At the same time the E-plane radiation pattern is broadened and the beamwidths become essentially equal in all planes. A measured E-plane pattern for linear polarization is shown in Fig. 2. The corresponding H-plane pattern is identical down to the −20-dB points, then shows first sidelobes peaking at −24 dB. In the 45° planes there are no sidelobes visible above −40 dB. The half-power beamwidth is 20.5°, hence footprint diameter from altitude H is approximately $0.36H$.

Beam efficiency as a function of angle from beam peak is shown in Fig. 3, and is seen to rise very rapidly, reaching essentially 98 percent at the −20-dB point. Fig. 3 is based upon computer calculations of the quantity

$$\eta(\theta) = \int_0^{\theta} P(\theta) \sin\theta \, d\theta \Big/ \int_0^{\pi} P(\theta) \sin\theta \, d\theta$$

where $P(\theta)$ is the average of the experimentally measured E- and H-plane patterns.

Circular polarization is created by use of a carefully matched Teflon slab inserted diagonally in the square waveguide feeding the horn.

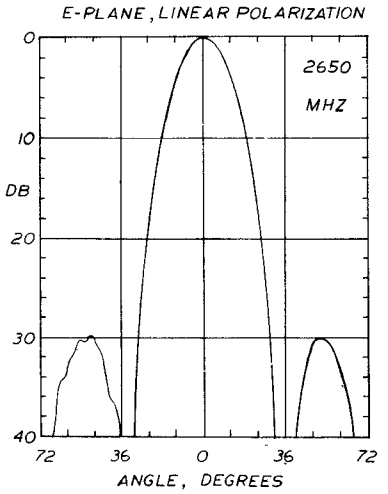

Fig. 2. Antenna E-plane pattern.

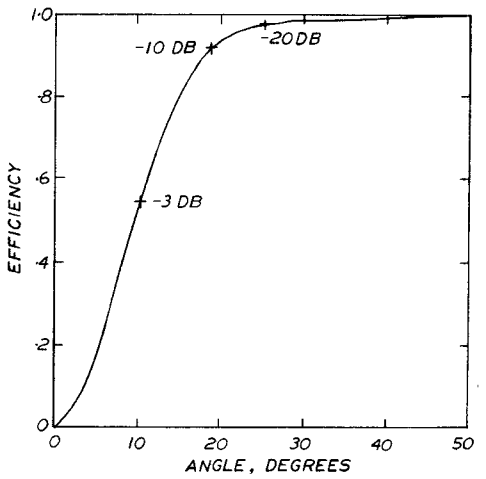

Fig. 3. Antenna beam efficiency.

B. Microwave Integrated Circuit (MIC)

The components shown enclosed in the hatched area of Fig. 1 have been fabricated in microstripline on substrates of high-purity alumina and placed on opposing broad walls of a short length of rectangular waveguide of standard dimensions, 2.84 by 1.34 in. Coupling to the waveguide is by means of probes as indicated schematically in Fig. 4, and the physical separation of the signal circuit from the noise injection circuit ensures that no spurious coupling exists between the two circuits. The relatively large signal probe is rigidly held inside a beryllia tube that, in turn, is captivated between the waveguide walls. Its coupling factor is unity since it is matched by adjustment of its length and location relative to the waveguide short circuit. The noise injection probe is short and couples weakly (−20 dB) in a bidirectional manner to the guide. Although the argument in Section II assumed use of a directional coupler, the conclusions therein are still valid; only the algebraic details are affected by use of bidirectional coupling.

The waveguide structure is machined from two blocks of aluminum that are later mated together along with a third block forming a short-circuiting plug in the waveguide. The whole assembly is then dip brazed, resulting in a short length of seamless low-loss waveguide. Fig. 5 shows the stripline signal circuit mounted in a cavity in the aluminum block. The circulator switch is of the latching type and is switched by applying a pulse to a center-tapped coil wound on a ferrite yoke. Pulse energy is less than 800 μJ and heating of the ferrite circulator puck is negligible. A second circulator acts as an isolator and the signal output is via a type SMA 50-Ω connector on the side of the block.

The noise injection circuit is in microstrip and is similarly housed in a cavity on the other side of the block. The avalanche diode chip is operated at constant regulated reverse current of about 0.7 mA and generates 36-dB excess noise. Tests show that the noise output of such diodes is stable to 0.001 dB/day and 0.0015 dB/week when operated at constant current in an environment controlled to 0.05 K in temperature.

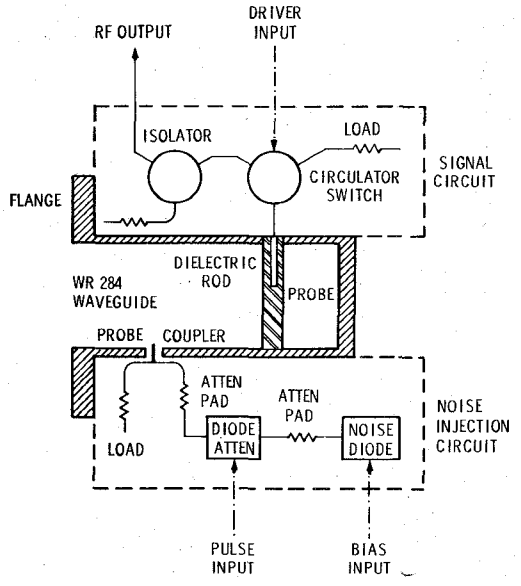

Fig. 4. Schematic of MIC.

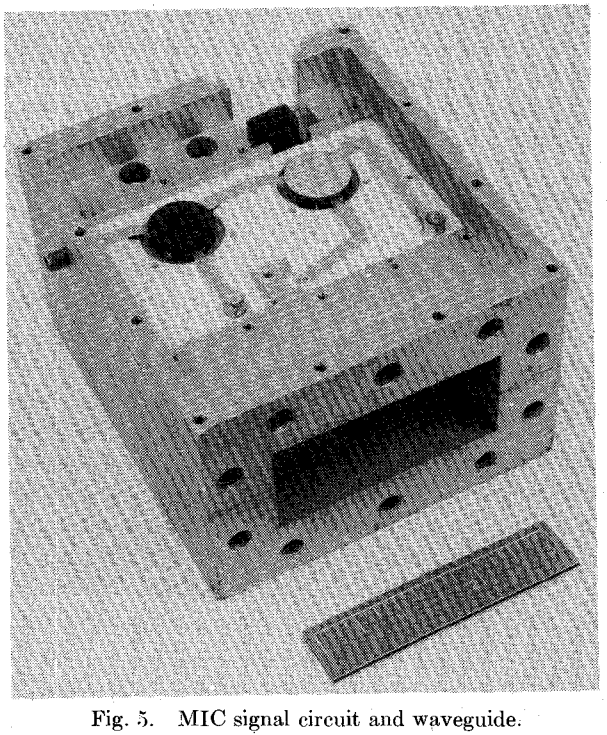

Fig. 5. MIC signal circuit and waveguide.

The diode switch consists of two diodes spaced $\lambda/4$ apart in the microstrip line and isolated by 6-dB attenuator pads from the noise diode and the −20-dB coupling probe. Switch isolation exceeds 50 dB and equivalent noise leakage is negligible at the radiometer input. The line beyond the probe (Fig. 4) is terminated in a 50-Ω pill package.

The face of the waveguide block shown in Fig. 5 is connected to the square-waveguide horn input by means of a two-section $\lambda_g/4$ transformer that serves to match the 1.34- by 2.84-in rectangular guide to the 2.84-in square guide. Both sections of the transformer have walls of thin (0.020-in) stainless steel, gold plated to reduce loss. Thus the transformer acts as an excellent thermal insulator between the temperature-regulated MIC and the unregulated antenna. Radiative and convective heat transfer are effectively blocked by two thin plugs of foamed polystyrene placed in each of the transformer sections. The small reflections from the plugs cancel, since they are spaced $\lambda_g/4$ apart.

The MIC and transformer assembly is housed in an insulated package using a 2-in thickness of Styrofoam on all sides except that on which the transformer joins the antenna. Two strip heating elements are located in the signal circuit cavity and two more in the noise injection cavity. A thermistor temperature-sensing element, mounted in the signal circuit cavity, is used with a commercial proportional temperature controller to supply power to the heater elements. Tests show that the whole enclosure can be maintained at 10°C above ambient with stability better than 0.03 K. About 8 W of heating power is initially used to bring the enclosure to its 10° excess temperature. Only 1 W is needed thereafter to maintain regulation.

The temperature controller exercises control but does not measure temperature. An additional sensor is needed for this purpose and a type FDN 600 silicon diode is mounted adjacent to the reference termination of the circulator switch. The diode is forward biased with a constant current of approximately 10 μA and has a linear voltage drop with slope of −2.8 mV/K. Such diodes are very useful as temperature sensors, being very stable and many times more sensitive than thermocouples, but they require calibration.

C. Receiver

This portion of the radiometer comprises the parametric amplifier, mixer/IF amplifier, square-law detector, and low-noise AF amplifier shown in the simplified block diagram, Fig. 1. These components, plus filters, pads, and isolators, are all firmly mounted to an aluminum-base plate and enclosed in an insulated box that is thermostatically controlled in temperature to ±1°C. A 2600–2700 MHz bandpass filter is used ahead of the paramp to limit out of band radar interference. The paramp operates degenerately, being pumped at twice the signal frequency, 2650 MHz, and provides gain of 20 dB. Gain stabilization is accomplished by sensing varactor current changes. These are used to control pump power (by means of a p-i-n diode attenuator) in such a way as to oppose the changes. The stabilization is particularly effective in suppressing gain fluctuations that might occur at the 50-Hz modulation frequency, these being the only form of fluctuations to which the radiometer is sensitive.

The local oscillator frequency is equal to the signal frequency, 2650 MHz; hence the double-balanced mixer down converts the signal to zero IF frequency. The passband of the IF amplifier extends from about 200 kHz to well over 50 MHz. Low-frequency response is deliberately cut off to suppress excess low-frequency noise, but little loss in information bandwidth occurs. The RF bandwidth is defined by a low-pass filter following the IF amplifier,

having a very sharp cutoff at 50 MHz. Because negative frequencies are folded over, due to the zero IF frequency, the effective input RF bandwidth is 100 MHz.

Detection is accomplished by a hot carrier Schottky diode, selected for its very low $1/f$ noise characteristic. The diode is operated at 20-μA forward bias, and the RF input signal level is carefully restricted to ensure that the detection characteristic does not deviate from square law by more than 2 parts in 10^3 (see Appendix). The detected 50-Hz pseudo square-wave amplitude is correspondingly small and necessitates extreme care in the design of the following audio amplifier. A low-noise FET input stage is used, followed by a low-noise operational amplifier. The passband is from about 2 Hz to 1 kHz in order to preserve the pseudo square-wave shape of the signal.

Pump and local oscillator signals are derived from a solid-state source comprising crystal controlled oscillator and multiplier chain.

D. Low-Frequency Electronics

Following audio amplification, the 50-Hz ac signal is synchronously demodulated, yielding a noisy dc error signal that is smoothed by an operational amplifier integrator. The smoothed dc voltage is then applied as the input to a precision switching integrator whose output is accurately constrained to lie between two predetermined voltage levels. The integrator output rises at a rate determined by the dc input voltage until it reaches the preset bound. At this instant the dc input is inverted and the output falls at the same rate until the lower bound is reached. The output is thus a triangular wave whose frequency is proportional to the input dc voltage.

The triangular wave is suitably processed and used to trigger a monostable multivibrator (the pulse generator in Fig. 1) whose output consists of 40-μs-wide pulses at a repetition frequency varying from 0 to about 13 kHz. A line driver is then used to apply these pulses to the pair of switching diodes in the noise injection circuit of the MIC.

In Section II it was shown that the overall stability and accuracy of the radiometer depend directly on the stability of the pulsewidth τ. This places very stringent requirements on the pulse generator, demanding constancy in the width of the 40-μs pulses to 1 part in 10^4. To alleviate this situation and at the same time to obtain an analog voltage instead of digital pulse output, an alternative technique has been devised. Instead of measuring the frequency of the pulses, the switching waveform for the diode switch is used to generate pulses of very high amplitude stability. This is done by use of low saturation resistance FET's to switch a high impedance load (0.5 MΩ) from zero voltage to a precision -2-V supply, regulated to ± 1 part in 10^4. The resulting pulses, which are all of the same amplitude, are averaged by a low-pass filter with time constant of about 1 s. To the extent that the precision pulses follow the switching of the avalanche noise diode, the output voltage $-V$ of the low-pass filter is rigorously proportional to the average injected noise power, independent of the pulsewidth. Additional precision analog operations are then used to form a voltage output that represents T_A, as given by (12), with a scale factor of precisely 100°/V. Due to differences in rise and fall times at various points in the circuitry, the precision pulses have a slightly different width than the microwave noise pulses. Under these conditions the pulsewidth still must be kept fairly constant, but the stability requirement is at least an order of magnitude less stringent.

V. CALIBRATION

Calibration consists in establishing a known temperature T_c at the horn aperture. This eliminates the need for highly uncertain corrections that would otherwise be required because of the differences in ohmic and mismatch losses between antenna and calibrating termination. It is clear from Section III that only one calibrating temperature is needed, for the system is linear and the second point is established by the precision reference temperature T_0.

The calibrating device used for this purpose is termed a cryoload, and is shown in Fig. 6. It must be regarded as a primary standard of brightness whose temperature can be accurately calculated. The justification for this statement, along with a more complete description of the device, is given elsewhere [11]. Suffice it to say here that the porous pyramidal microwave absorber is totally saturated with a boiling cryogen. Liquid nitrogen is usually used, with a boiling point of $77.36 + 0.011\ (p\text{-}760)$ K, where p is the barometric pressure in millimeters of mercury.

The pyramidal absorber is held in place by a conformal cap of nonporous low-loss polyurethane foam having a dielectric constant of 1.2. This cap further serves the purpose of confining the cryogenic liquid to the tapered absorber material, thereby avoiding the relatively large reflection coefficient of a liquid interface. Small vent holes drilled through the foam at the absorber tips enable the cryogenic vapor to escape. The assembly is housed in a leakproof aluminum tank surrounded by thick insulating walls of Styrofoam.

The calibrating temperature T_c is calculated by adding two small corrections to the liquid nitrogen boiling point given above. These corrections, which total 0.1 K, account for the small reflection occurring at the polyurethane foam surface and for the fact that the antenna does not couple entirely to the cryoload alone. Coupling to external space, however, is down by at least 40 dB due to the use of foil shielding, as shown in Fig. 6. The foil is actually aluminum-coated Mylar film and attaches readily to the flange at the horn aperture by means of stainless-steel Velcro.

VI. RESULTS

The total RF loss through the microwave integrated circuit is 1.0 dB and the IF bandwidth is 50 MHz. Thus (14) predicts rms fluctuations of magnitude 0.09 K for a response time of 1 s. Experimentally, the fluctuations were observed to be almost exactly 0.09 K. This seems to

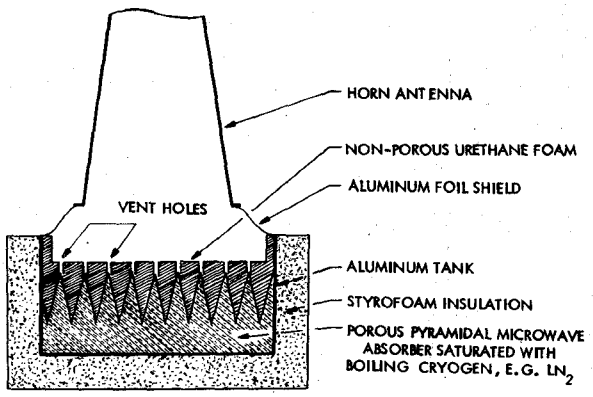

Fig. 6. Antenna cryoload.

show that "quantization" noise caused by the finite number of pulses occurring in each half of the modulation cycle is negligible.

The initial performance tests on the radiometer comprised calibration and stability tests at 77.4 K using liquid nitrogen in the cryoload, followed by checks using liquid argon (at 87.3 K), at room temperature, and finally, a measurement of the zenith sky temperature at night. The measured stability was observed to be 0.1 K/day, and was better than 0.3 K over a 1-week period. The results of the argon and room temperature tests were within 0.1 K of the boiling point and the thermometric temperature, respectively. The room temperature results are evidence that no significant offset errors exist, such as might be caused by spurious noise diode leakage. The sky measurement gave a brightness temperature of 4.8 K at the zenith.

Following these tests the instrument was completely dismantled and shipped to another laboratory where it underwent stringent environmental testing, including temperature cycling, vibration, and shock. Upon completion of environmental tests and subsequent reassembly, the same series of performance tests described previously was repeated. It is noteworthy that the instrument was found to be out of calibration by only 0.3 K at the end of the 5-week environmental testing period. A slight adjustment was made to correct the calibration before repeating the tests. The results were then identical to the first tests, described previously.

Tests using nitrogen and argon in the cryoload have been repeated a number of times since the instrument's installation in a NASA aircraft at Wallops Station, Va. Stability and repeatability of at least 0.3 K were observed on each occasion, with one exception. In that case a calibration drift of 0.7 K at the end of a week was observed, but it appears this was due to improper use of the cryoload.

Theoretical calculations of zenith sky temperature give the value 5.2 $\pm$ 0.5 K, including contributions by oxygen absorption in the atmosphere and galactic and cosmic background emission integrated over the horn antenna radiation pattern. The observed temperature 4.8 K is in good agreement with this value and is an indication of the high absolute precision and linearity of the radiometer.

VII. CONCLUSIONS

A novel radiometer system has been developed that aims at high absolute accuracy and linearity. Such a radiometer has been constructed for use at *S* band and has been thoroughly tested. The instrument is extremely linear over its measurement range 0–300 K, and possesses excellent long-term stability (<0.3 K/week). For target-source temperatures around 100 K (i.e., not too different from the calibrating temperature T_c) the radiometer has demonstrated an absolute accuracy approaching 0.1 K.

It is compact and robust, consumes little power, and is potentially suitable for use in a satellite since it uses no cryogen during operation. In polar orbit, the instrument is capable of remotely measuring the sea surface thermal emission over the entire earth to an accuracy approaching 0.1 percent.

The performance of the total radiometer demonstrates an upper limit to the long-term stability of solid-state avalanche noise diodes of better than $\pm$0.0015 dB/week.

APPENDIX

Effect of Departure from Square-Law Detection

It is important to investigate the error that arises as a result of departure from square-law response by the diode detector. If the RF power level incident on the diode is expressed as a temperature T, referred to the input of the parametric amplifier, then the ac output voltage of the detector may be written as

$$e_{out} = CT(1 + \mu T + \cdots) \tag{A.1}$$

where C is a constant of the system and μT represents the deviation from square-law response.

During one period of the modulation cycle the power level T will assume the following three different values:

$$\begin{aligned} T_1 &= (1 - \beta)T_A + \beta T_0 + T_R \\ T_2 &= (1 - \beta)T_A + \beta T_e + \beta T_0 + T_R \\ T_3 &= T_0 + T_R \end{aligned} \tag{A.2}$$

where all quantities are as defined in Section III. T_1 and T_2 represent conditions during the pulse off and pulse on times, respectively, while T_3 is the reference condition.

If ideal square-law detection is assumed (i.e., $\mu = 0$), then the null condition is simply

$$T_3 = f_T T_2 + (1 - f_T)T_1 \tag{A.3}$$

and substitution of (A.2) in (A.3) leads to

$$T_A = T_0 - \frac{f}{f_c}(T_0 - T_c) \tag{A.4}$$

which is exactly the radiometer transfer equation given by (12).

In practice, μ is small but finite, and the true null condition is in reality given by

$$e_3 = f_T e_2 + (1 - f_T)e_1 \tag{A.5}$$

whence

$$f\tau = \frac{e_3 - e_1}{e_2 - e_1}. \tag{A.6}$$

Upon substitution of (A.1), making use of the approximation that μT is small, it is found that

$$f\tau \simeq \frac{T_3 - T_1}{T_2 - T_1}[1 + \mu(T_3 - T_2)]. \tag{A.7}$$

Using (A.2) in (A.7) and again approximating to first order in μT, one obtains

$$\frac{f}{f_c} \simeq \frac{T_0 - T_A}{T_0 - T_c} \cdot [1 - \mu(1 - \beta)(T_A - T_c)]. \tag{A.8}$$

If (A.4) is used to obtain an apparent temperature, then

$$(T_A)_{\text{apparent}} = T_A + \mu(1 - \beta)(T_A - T_c)(T_0 - T_A). \tag{A.9}$$

Defining a fractional square-law deviation factor δ by means of

$$\delta = \mu(T_0 + T_R) \tag{A.10}$$

and making the approximation that $1 - \beta$ is essentially unity (-20-dB coupling factor), the error in T_A can be written

$$\Delta T_A = -\delta \frac{(T_0 - T_A)(T_A - T_c)}{T_0 + T_R}. \tag{A.11}$$

As would be expected, the error is small whenever T_A is close to either the calibrating temperature T_c or the reference temperature T_0. For values appropriate to this radiometer, namely, $T_0 = 300$ K, $T_A = 110$ K, $T_c = 78$ K, and $T_R = 70$ K, the error will be less than 0.03 K, providing the deviation factor δ does not exceed 2×10^{-3}.

An analysis of the detection process of the hot carrier diode, based on the work of Cowley and Sorensen [12], shows the following, provided the diode is fed by a low impedance source, e.g., a few ohms.

1) The deviation from square-law response is independent of bias current and is given by $\delta = u^2A^2/16$, where A is the peak RF voltage and $u \approx e/kT$, or $(26\text{ mV})^{-1}$.

2) The voltage sensitivity of the diode is also independent of bias current.

3) The diode noise decreases with increasing bias current until $1/f$ noise dominates and a constant level is observed.

4) In the bias region of constant noise the signal to noise (S/N) ratio is proportional to δ, the square-law deviation factor, and the detected output signal voltage is equal to $4\delta/u$, or approximately 100δ mV.

As a practical procedure, then, the diode bias current is increased until no further decrease in noise is observed. This occurs at a bias level of about 20 μA for the type HP5082 diode used here, and results in a video impedance of 1300 Ω. Finally, to ensure that the deviation from square-law response does not exceed 2 parts in 10^3, the RF gain is adjusted in accordance with 4) to limit the detected output to 200 μV.

ACKNOWLEDGMENT

The authors wish to thank L. A. Ahlberg, M. J. Van Melle, and H. H. Wang for their excellent experimental assistance throughout, and H. Morgan and L. Struve for their later contributions. They also wish to thank H. J. C. Blume of NASA Langley Research Center for his advice and cooperation.

REFERENCES

[1] R. H. Dicke, "The measurement of thermal radiation at microwave frequencies," *Rev. Sci. Instrum.*, vol. 17, pp. 268–275, July 1946.
[2] G. M. Hidy *et al.*, "Development of a satellite microwave radiometer to sense the surface temperature of the world oceans," NASA Contractor Rep. NASA CR-1960, Feb. 1972.
[3] A. Stogryn, "The apparent temperature of the sea at microwave frequencies," *IEEE Trans. Antennas Propagat.*, vol. AP-15, pp. 278–286, Mar. 1967.
[4] A. Van Der Ziel, *Noise*. Englewood Cliffs, N. J.: Prentice-Hall, 1954.
[5] W. B. Goggins, Jr., "A microwave feedback radiometer," *IEEE Trans. Aerospace Electron. Syst.*, vol. AES-3, pp. 83–90, Jan. 1967.
[6] T. V. Seling, "An investigation of a feedback control system for stabilization of microwave radiometers," *IRE Trans. Microwave Theory Tech.*, vol. MTT-10, pp. 209–213, May 1962.
[7] M. E. Tiuri, "Radio astronomy receivers," *IEEE Trans. Antennas Propagat.*, vol. AP-12, pp. 930–938, Dec. 1964.
[8] W. F. Bahret and L. Peters, Jr., "Small-aperture small-flare-angle corrugated horns," *IEEE Trans. Antennas Propagat.* (Communications), vol. AP-16, pp. 494–495, July 1968.
[9] P. D. Potter, "A new horn antenna with suppressed sidelobes and equal beamwidths," *Microwave J.*, vol. 6, pp. 71–78, June 1963.
[10] S. B. Cohn, "Flare angle changes in a horn as a means of pattern control," *Microwave J.*, vol. 13, pp. 41–46, Oct. 1970.
[11] W. N. Hardy, "Precision temperature reference for microwave radiometry," *IEEE Trans. Microwave Theory Tech.* (Short Papers), vol. MTT-21, pp. 149–150, Mar. 1973.
[12] A. M. Cowley and H. O. Sorensen, "Quantitative comparison of solid-state microwave detectors," *IEEE Trans. Microwave Theory Tech. (1966 Symposium Issue)*, vol. MTT-14, pp. 588–602, Dec. 1966.